Smart Structures and Systems, *Vol. 26, No. 2 (2020) 135-146*
DOI: https://doi.org/10.12989/sss.2020.26.2.135

Online structural identification by Teager Energy Operator and blind source separation

Vida Ghasemi [a] and Fereidoun Amini*

Department of Civil Engineering, Iran University of Science and Technology, Narmak, Tehran, Iran

(*Received October 20, 2018, Revised June 3, 2020, Accepted June 28, 2020*)

Abstract. This paper deals with an application of adaptive blind source separation (BSS) method, equivariant adaptive separation via independence (EASI), and Teager Energy Operator (TEO) for online identification of structural modal parameters. The aim of adaptive BSS methods is recovering a set of independent sources from their unknown linear mixtures in each step when a new sample is received. In the proposed approach, firstly, the EASI method is used to decompose structural responses into independent sources at each instance. Secondly, the TEO based demodulation method with discrete energy separation algorithm (DESA-1) is applied to each independent source, and the instantaneous frequencies and damping ratios are extracted. The DESA-1 method can provide the fast time response and has high resolution so it is suitable for online problems. This paper also compares the performance of DESA-1 algorithm with Hilbert transform (HT) method. Compared to HT method, the DESA-1 method requires smaller amounts of samples to estimate and has a smaller computational complexity and faster adaption due to instantaneous characteristic. Furthermore, due to high resolution of the DESA-1 algorithm, it is very sensitive to noise and outliers. The effectiveness of the proposed approach has been validated using synthetic examples and a benchmark structure.

Keywords: adaptive blind source separation; discrete energy separation algorithm; equivariant adaptive separation via independence algorithm; online structural identification; Teager-Energy Operator

1. Introduction

Recent seismic disasters, all over the world show the importance of controlling structures and preventing structural damage. Online system identification (SI) has a key role in controlling structures against environmental excitations, such as earthquakes and wind forces and one of the main objectives of structural health monitoring (SHM) is to detect damages in structures in real time. Therefore, online SI and structural health monitoring (SHM) have received considerable attention over the last decades and many methods have been introduced and presented. Chase *et al*. (2005a, b) used the adaptive RLS filtering technique and the adaptive least mean square filtering technique for identification of structural parameters. Also, Shih employed an on-line recursive least-squares (RLS) technique to identify the time-varying dynamic parameters of structures (Chu and Lo 2011). The two singular value decomposition (SVD) and QR decomposition techniques are commonly the most used methods in offline SI. They have been adopted for online SI by operating on moving time windows of fixed lengths: when a new data is observed, the subspace identification is updated (Loh *et al*. 2011). Also, recursive Bayesian filters are used by Azam *et al*. (Azam *et al*. 2017, Azam and Mariani 2018) to detect damage in real-time by means of joint estimation of state and stiffness parameters. Adaptive Kalman filters have been widely applied for state estimation, parameter estimation and joint state-parameter estimation. These methods are classified as recursive methods and through updating structural state/parameter recursively can be applied for online system identification (Song *et al*. 2020). Machine learning algorithms have been also used to detect structural damages in recent years (Santos *et al*. 2016). Rageh *et al*. (2020) employed machine learning algorithms for damage detection in steel railway bridges. In their proposed algorithm Proper Orthogonal Decomposition (POD) and Artificial Neural Networks (ANNs) have been used to identify damage location and intensity under train loads.

In recent decades, the output-only system identification methods (Ramazani and Bahar 2015, McNeill and Zimmerman 2008, Loh *et al*. 2012) such as blind source separation methods (BSS) (Sadhu *et al*. 2014, Nagarajaiah and Yang 2015) have received attention. The goal of BSS is recovering the sources from a mixture of output measurements without any prior information about the source signals or the mixing process. Among BSS methods, the independent component analysis (ICA) and the second-order blind identification (SOBI) (Poncelet *et al*. 2007, Rainieri 2014) are most popular.

Most of BSS algorithms are based on the assumption of the stationary excitation. However, some researchers effort to develop BSS methods for non-stationary excitations (Hazra *et al*. 2010, Abazarsa *et al*. 2016). Ghahari *et al*. (2017) demonstrated BSS method can be used for system identification when we deal with unknown and

*Corresponding author, Ph.D., Professor,
E-mail: famini@iust.ac.ir
[a] Ph.D. Student, E-mail: vida.ghasemi62@gmail.com

ISSN: 1738-1584 (Print), 1738-1991 (Online)

nonstationary inputs. They use generalized eigen-decomposition and rough-fuzzy c-means clustering techniques together for identifying the mode shapes. Non-stationary data may vary frequency contents and lead to inaccurate separation. To overcome disadvantages caused by non-stationary excitations, Guo and Kareem (2016a) have proposed novel method based on Time-Frequency Blind Source Separation (TFBSS) using spatial time-frequency distribution (STFD).

Traditional BSS methods require batch data for the separation, so these algorithm aren't proper for online problems when new samples are received one after another. Utilization of offline BSS methods for online problems wastes a good amount of time. As the size of relevant matrices and vectors increases with the number of given data, so does the analysis time (Amini and Ghasemi 2018). To overcome these disadvantage online BSS methods have been introduced for separation.

Jutten and Herault (1991) initially proposed an adaptive BSS, followed by another method based on neural network architecture (Sorouchyari 1991). Cardoso and Laheld (1996) used the 'relative gradient' adaptive algorithm based on serial updating to update the separating matrix in each step when a new sample is received. The proposed adaptive algorithm is called equivariant adaptive separation via independence (EASI). Dependence of the convergence on source statistics (Jutten and Herault 1991, Comon 1989) and complexities of analysis (Comon 1989, Lagunas Hernandez 1994) are two main drawbacks of the EASI algorithm.

A novel method was introduced by Zarzoso and Nandi (2000) to overcome these disadvantages. Also, different adaptive BSS methods to improve the available algorithms were developed by some researchers (Samadi *et al*. 2004). Reference (Ye and Jin 2009) proposed an optimized EASI algorithm to increase the convergence speed. In Ref. (Amini and Ghasemi 2018) EASI algorithm has been applied for structural systems. For each time step, the modal matrix and modal coordinates of the structure are extracted using the EASI algorithm, based only on structural output responses received online. In this paper, the DESA-1algorihtm is combined with the EASI algorithm to apply on modal coordinates for identifying modal parameters in real time.

There are some methods for frequency estimation. The well-known methods are the short time Fourier transformation (STFT) (Guo and Kareem 2016b) and Hilbert transform (HT) (Feldman 2011). As disadvantageous fact, both methods lead to a bad resolution. Because of the limited observation length of the signal instead of mentioned methods other approaches are utilized to determine the instantaneous frequency.

One of the main approaches in order to obtain the instantaneous frequency and amplitude of real-valued signals is to use Energy Separation Algorithm (Maragos *et al*. 1993, Liang and Bozchalooi 2010). This method is based on the nonlinear differential Teager Energy Operator (TEO) (Kaiser 1990). The length of the computing window is small in the Teager Energy Operator (TEO) so it is suitable for real-time and online problems. At first, TEO developed for a speech production modeling. Then, Maragos introduced a discrete energy separation algorithm (DESA-1) based on TEO to provide instantaneous frequencies and amplitudes of signals. The DESA-1 separates a signal into its amplitude modulating (AM) and frequency modulating (FM) components. TEO and DESA-1 have been used in signal processing for demodulation (Dimitriadis and Maragos 2006). Recently, TEO has been applied in fault detection (Sadhu *et al*. 2016, Azergui *et al*. 2018), SHM and damage detection (Cao *et al*. 2014, Ulriksen and Damkilde 2016).

In this paper, the Teager energy operator demodulation method and EASI method are combined for online modal identification of the structures. The conjunction of these two methods is called EASI-Teager approach. In the beginning, the EASI algorithm is applied to structural output responses which are received online in order to extract modal matrix and modal coordinates. In free vibration case, the extracted modal coordinates are sinusoidal signals and parameter estimation is easy. But for forced vibration, the extracted modal coordinates don't follow sinusoidal form; this issue makes identification very difficult. To overcome this problem, natural excitation technique (NExT) is proposed. This technique developed by James *et al*. (1993) to obtain signals with the same characteristics as free response data from ambient vibration.

Then the instantaneous frequencies and damping ratios are estimated from information hidden in the modal coordinates by using DESA-1 algorithm. The performance of DESA-1 algorithm is compared with HT method. The results shows the DESA-1 has high resolution, smaller computational complexity and faster adaption due to instantaneous nature.

In addition, according to the results. Main disadvantage of the DESA-1 algorithm is its sensitivity to presence of noise and outliers due to high resolution. Depending on the amount of noise, it may deteriorate the DESA-1 efficiency. Consequently, in order to achieve accurate results, median filter is used to remove outliers from the data.

The efficacy of the mentioned algorithm is investigated utilizing synthetic example simulation studies. The phase I IASC-ASCE benchmark building is used for verification of this method as well. Results show that the EASI-Teager algorithm is efficient and proper for online structural identification. In this study, in spite of the fact that, in numerical simulations and benchmark, the responses are batch, but in order to simulate online identification, it is assumed new data is recorded for each time so it is used one by one.

The reminder of this paper is organized as follows: In section 2, the problem statement is presented. The EASI and DESA-1 algorithms are formulated for structural identification in sections 3 and 4, respectively. Comparison between DESA-1 and HT methods are performed in section 5. In section 6, the robustness of proposed algorithm with respect to noise and outliers are investigated. The proposed EASI-Teager method is presented in section 7. Numerical simulation of (2-DOF) shear-beam building for evaluating the performance of the proposed method is described in section 8. In section 9, the performance of the proposed method is addressed using the phase I IASC-ASCE

benchmark building. Finally, section 10 concludes the paper.

2. Formulation for proposed approach

For a linear and lumped-mass n-degree-of-freedom (n-DOF) structural system under an excitation force vector $\mathbf{f}(t)$, the governing differential equations can be written as Eq. (1).

$$\mathbf{M}\ddot{\mathbf{x}}(t) + \mathbf{C}\dot{\mathbf{x}}(t) + \mathbf{K}\mathbf{x}(t) = \mathbf{f}(t) \tag{1}$$

Where M, C and K are symmetric mass, damping and stiffness matrices, respectively. $\mathbf{x}(t)$, $\dot{\mathbf{x}}(t)$ and $\ddot{\mathbf{x}}(t)$ are the displacement, velocity and acceleration vectors, respectively. For proportionally damped systems, the displacement responses can be expressed in modal space as Eq. (2).

$$\mathrm{x} = \Phi \mathrm{q} \tag{2}$$

Where $\mathbf{\Phi} \in \mathbb{R}^{n\times n}$ and $\mathbf{q} \in \mathbb{R}^{n\times 1}$ are the modal matrix and modal coordinate vector respectively. For stationary white noise excitations the $q_j(t)$ modal coordinate is expressed as Eq. (3).

$$\begin{aligned} q_j(t) &= \alpha_j e^{\zeta_j \omega_j t} \sin\left(\omega_{dj} t + \theta_j\right), \\ \omega_{dj} &= \omega_j (1-\zeta_j^2)^{1/2} \end{aligned} \tag{3}$$

Where ζ_j, ω_j, ω_{dj}, θ_j and α_j are damping ratio, natural modal frequency, damped modal frequency, phase lag and constant parameter, respectively.

3. Adaptive blind source separation and EASI algorithm

Blind source separation (BSS) consists in separating the source signals from observed linear mixtures without resorting to any a priori information about mixing matrix. The BSS model is formulated as Eq. (4).

$$\mathbf{x}(t) = \mathbf{A}\mathbf{s}(t) \tag{4}$$

Where $\mathbf{x}(t) = [x_1(t),\ x_2(t), \dots, x_m(t)]^T \in \mathbb{R}^m$ is a vector of measured signals, $\mathbf{A} \in \mathbb{R}^{m\times n}$ is an unknown mixing matrix and $\mathbf{s}(t) = [s_1(t),\ s_2(t), \dots, s_n(t)]^T \in \mathbb{R}^n$ is a source vector. When the modal coordinates are mutually uncorrelated, they can be considered as independent sources and subsequently the modal identification of structures lies within the framework of BSS problem.

In online problems, due to a lack of whole complete response signals, adaptive methods are used. The schematic illustration of an adaptive BSS is shown in Fig. 1 (Cardoso and Laheld 1996).

In adaptive source separation, the separating matrix $\mathbf{B}_t$ is a time-varying matrix that is updated each time. One of the most useful iterative techniques for BSS is the Equivariant Adaptive Separation via Independence (EASI) which uses "serial updating" technique (Cardoso and Laheld 1996) for updating $\mathbf{B}_t$ according to Eq. (5).

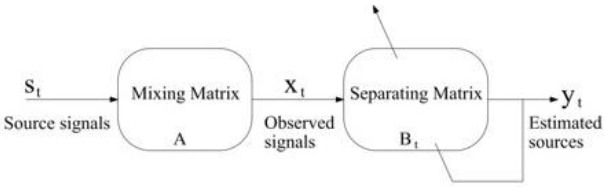

Fig. 1 Schematic illustration of an adaptive BSS

$$\mathbf{B}_{t+1} = \mathbf{B}_t - \lambda_t H(\mathbf{y}_t)\mathbf{B}_t \tag{5}$$

Where, $\mathbf{y}_t$ is the output of $\mathbf{B}_t$, function $H(\mathbf{y}_t)$ is determined such that $\mathbf{y} \to H(\mathbf{y})$ and λ_t is a sequence of positive adaption steps. Essential assumptions used in the EASI algorithm are described below:

a: Matrix $\mathbf{A}$ is full rank with $n \le m$.
b: Each component of $\mathbf{s}_t$ is a stationary zero mean process.
c: At each t, $\mathbf{s}_t$ components are mutually statistically independent.
d: $\mathbf{s}_t$ components have unit variance.

When the data is transformed to new data with uncorrelated components that equal unity in their variances it is said the new data is white and the transform matrix is called whitening matrix. The batch algorithms of BSS have two main stages as follows: determining of whitening matrix $\mathbf{W}$ and applying to the data, computing the orthogonal matrix U and applying to whited data and finally the separating matrix B is achieved as the product B = UW.

In the EASI algorithm, "relative gradient" technique is used to update a matrix $\mathbf{W}$ such that $\mathbf{W}\mathbf{R}_\mathbf{X}\mathbf{W}$ converge to unit matrix. Where $\mathbf{R}_\mathbf{x}$ is the covariance matrix of x. A serial update whitening algorithm is obtained as Eq. (6).

$$\mathbf{W}_{t+1} \overset{\text{def}}{=} \mathbf{W}_t - \lambda_t[\mathbf{z}_t\mathbf{z}_t^T]\mathbf{W}_t \tag{6}$$

Where $\mathbf{z}_t$ is whited data and $\mathbf{W}_t$ is whitening matrix in time t.

Then orthogonal matrix U is update such that the contrast function is minimized. A serial updating of orthogonal matrix U is obtained as Eq. (7)

$$\mathbf{U}_{t+1} \overset{\text{def}}{=} \mathbf{U}_t - \boldsymbol{\lambda}_t[\boldsymbol{H}(\mathbf{y}_t) - \boldsymbol{H}(\mathbf{y}_t)^T]\mathbf{U}_t \tag{7}$$

The function $H(\mathbf{y}_t)$ can be considered as follows

$$\boldsymbol{H}(\mathbf{y}) = \boldsymbol{g}(\mathbf{y})\mathbf{y}^T - \mathbf{y}\boldsymbol{g}(\mathbf{y})^T \tag{8}$$

Where $g(\mathbf{y}) = [g_1(y_1), \dots, g_n(y_n)]^T$ is component-wise arbitrary nonlinear function. According to Eq. (5) and Eq. (8), EASI algorithm for Adaptive Source Separation is obtained as Eq. (9).

$$\mathbf{B}_{t+1} = \mathbf{B}_t - \lambda_t[\mathbf{y}_t\mathbf{y}_t^T - \mathbf{I} + g(\mathbf{y}_t)\mathbf{y}_t^T - \mathbf{y}_t g(\mathbf{y}_t)^T]\mathbf{B}_t \tag{9}$$

4. Discrete energy separation algorithm

In this section, the discrete time Energy Separation Algorithm (DESA-1) (Maragos *et al*. 1993) is introduced to

online estimation of modal parameters. This algorithm is based on the Teager energy operator (TEO), which was derived by Kaiser in 1990 to measure the energy of the mechanical process. The TEO for continuous time signal $s(t)$ is

$$\Psi[s(t)] = [\dot{s}(t)]^2 - s(t)\ddot{s}(t) \quad (10)$$

Where $\dot{s}(t)$ and $\ddot{s}(t)$ are first and second derivatives of signal, respectively. $\Psi[.]$ denotes the Teager energy operator. For a discrete scheme, the TEO is defined as follows

$$\Psi[s_n] = {s_n}^2 - s_{n-1}.s_{n+1} \quad (11)$$

As shown in Eq. (11), only three samples are required for the energy computation at each time instant. Thus, the response of the TEO is fast and approximately instantaneous. Also, this issue makes it a high resolution energy estimator. The basic assumption in the DESA-1 algorithm is the positivity of the energy operator outputs.

Consider a signal with variable amplitude and variable frequency, given by the following

$$s_n = \rho_n cos\,(\Omega_n n + \theta) \quad (12)$$

Where ρ_n is the amplitude, Ω_n and θ are the digital frequency and arbitrary initial phase, respectively. Also, n is the temporal sampling point.

In Ref. (Maragos *et al*. 1993), an alternative approach to estimate the amplitude, ρ_n, and frequency, Ω_n, of amplitude modulation and frequency modulation (AM-FM) signals is developed which is called DESA-1 algorithm. In this algorithm, the energy operator is applied on signal then separated into two parts, amplitude and frequency, by using energy separation algorithm (ESA). The amplitude and frequency based on DESA-1 algorithm are obtained by equations below.

$$\Delta s_n = s_n - s_{n-1} \quad (13)$$

$$\rho_n \cong \sqrt{\frac{\Psi[s_n]}{1 - \frac{\Psi[\Delta s_n] + \Psi[\Delta s_{n+1}]}{4\Psi[s_n]}}} \quad (14)$$

$$\Omega_n \cong cos^{-1}\left(1 - \frac{\Psi[\Delta s_n] + \Psi[\Delta s_{n+1}]}{4\Psi[s_n]}\right) \quad (15)$$

The algorithm allows estimating the parameters of periodic signals with a frequency not exceeding the Nyquist frequency. An exponentially damped sinusoidal signal is a special case of an AM signal. In structural systems, as shown in Eq. (3) we almost deal with signals, that its amplitudes decay exponentially with time and frequencies are constant as expressed in Eq. (16).

$$s_n^d = e^{-\zeta\Omega n}\rho\cos(\Omega_d n + \theta)\,; \quad \Omega_d = \Omega\sqrt{1-\zeta^2} \quad (16)$$

Ω_d is damped digital frequency. As stated in (Kaiser 1993), for constant scalar b and arbitrary functions h_n and k_n, these energy functions are obtained.

$$\Psi[e^{-bn}] = 0 \quad (17)$$

$$\Psi[k_n h_n] = k_n^2\Psi[h_n] + h_n^2\Psi[k_n] - \Psi[k_n]\Psi[h_n] \quad (18)$$

Using the above mentioned equations and Eq. (16), one can calculate the Teager energy for signal as follows: For clarification

$$\Psi[s_n^d] = e^{-2\zeta\Omega n}\Psi[\rho\cos\,(\Omega_d n + \theta)] \quad (19)$$

For constant ρ and Ω, the Teager energy for cosine signal (Maragos *et al*. 1993) is given by Eq. (20).

$$\Psi[\rho\, cos(\Omega n + \theta)] = \rho^2 sin^2[\Omega] \quad (20)$$

Thus, Eq. (19) can be rewritten as Eq. (21).

$$\Psi[s_n^d] = e^{-2\zeta\Omega n}\rho^2\sin^2[\Omega_d] \quad (21)$$

Therefore, the damping coefficient can be determined by Eq. (22).

$$\zeta = \frac{1}{2\Omega} ln\left(\frac{\Psi[s_{n-1}^d]}{\Psi[s_n^d]}\right) \; or \; \zeta = \frac{1}{\Omega} ln\left(\frac{\rho_{n-1}}{\rho_n}\right) \quad (22)$$

As a sequence, Eq. (15) and Eq. (22) provide the objective of the modal identification.

5. Comparison between HT and DESA-1 methods

In this section, classical estimator of the instantaneous frequency, Hilbert transform (HT), has been compared to a modern instantaneous frequency estimator, DESA-1 method. The comparison is performed from viewpoints: magnitude of estimation error, resolution, computational complexity and adaptability to instantaneous signal changes. To clarify these comparisons, an example of damped cosine signal is used in Eq. (23).

$$x(t) = e^{-(0.01*0.7071)t}\cos(0.7071t - 0.01) \quad (23)$$

For simulations, the time step and total times are considered 0.1 and 100 seconds, respectively.

5.1 Resolution

The DESA-1 algorithm needs constant 5 points for estimation, so has high resolution. Fig. 2 illustrates the number of points needed for HT method to correctly estimate the parameters. As seen, the HT method requires at least 120 points for accurate estimation. Therefore, compared to the DESA-1 algorithm, the HT has less resolution.

5.2 Accuracy

For investigation of accuracy of the DESA-1 and HT methods, Magnitude of estimation error for two methods is compared. The normalized mean square error (NMSE) of estimation for the two methods with respect to the length of

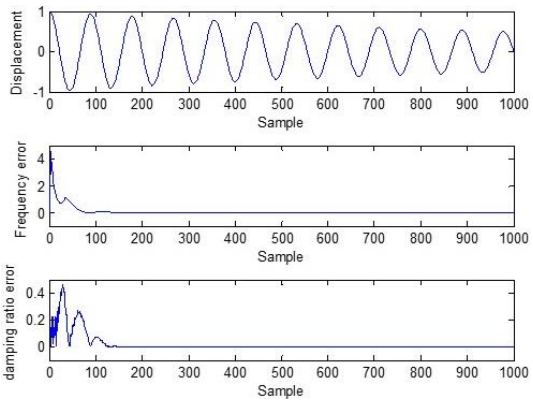

Fig. 2 Error of frequency and damping ratio estimation by HT method with respect to length of window for SDOF system

Table 1 Accuracy of the identification using HT and DESA-1 methods

Window Length	HT		DESA-1	
	NMSE of ω	NMSE of ζ	NMSE of ω	NMSE of ζ
$L = 100$	0.0142	29.0215	0.0000	0.0000
$L = 120$	0.0027	5.0031	0.0000	0.0000
$L = 150$	$7.55 * 10^{-5}$	0.0188	0.0000	0.0000
$L = 300$	$6.36 * 10^{-7}$	$5.93 * 10^{-5}$	0.0000	0.0000
$L = 500$	$2.69 * 10^{-9}$	$1.11 * 10^{-5}$	0.0000	0.0000

window for HT is presented in Table 1. The window and overlap lengths are denoted by W_L and $p = W_L - 1$, respectively.

From results, the HT method has good result for length of window greater than 150 points.

5.3 Adaptability

To target this issue, it is assumed in seconds 50, the signal specifications change and signal is given by the following equations

$$\begin{cases} x(t) = e^{-(0.01*0.7071)t}\cos(0.7071t - 0.01) & t \le 50 \\ x(t) = e^{-(0.03*0.6325)t}\cos(0.6322t + 0.8336) & t > 50 \end{cases} \quad (24)$$

AS shown in Fig. 3, due to system specification changes in seconds 50, the Teager energy of signal has been changed. It is clear; the DESA-1 is highly adaptable due to its high resolution.

5.4 Computational complexity

In Table 2, the computational complexity of HT and DESA-1 methods and the number of consecutive discrete signal samples to estimate the instantaneous frequency are presented. (The estimation of damping ratio is not included).

From Table 2, it is clear; the DESA-1 algorithm has smallest computational complexity and uses a smaller

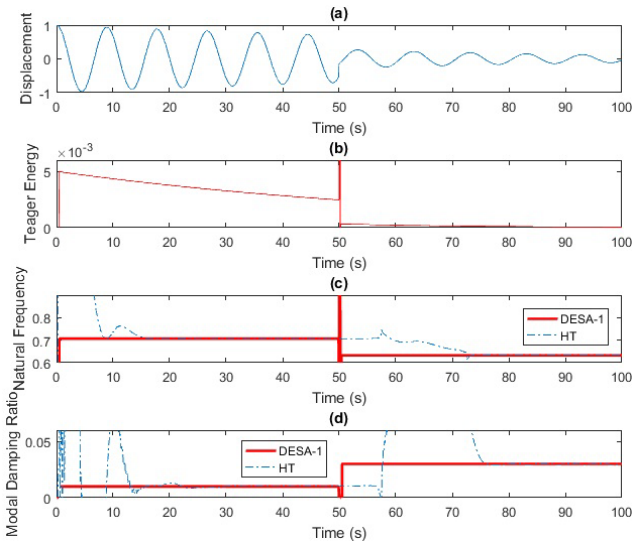

Fig. 3 Adaptability of DESA-1 and HT methods

Table 2 Computational complexity of HT and DESA-1 methods

Estimation	Method	Add/sub	Mul/Div	arccos (.)	$\sqrt{(.)}$	W_L
Frequency	HT	N+4	N+5	0	0	N
	DESA-1	5	6	1	0	5

number of samples compared to HT. In the following section, the effects of noise and outliers are investigated.

6. Robustness with respect to presence of noise and outliers

6.1 Effect of noise

In practical applications, output responses are always corrupted by noise. So it is important to see how well the DESA-1 performs in noisy environments. The basic assumption in the DESA-1 algorithm is that the operator outputs are always positive. In the absence of noise, the condition for the positivity of the operator outputs for pure sinusoidal inputs is established and the instantaneous property is also guaranteed. Noise has a severe impact on the performance of the DESA-1, mainly owning to the small number of samples used to estimate. Depending on the amount of noise, it may invalidate positivity of energy operator output and deteriorate the DESA-1 efficiency. This problem is investigated in the example introduced in Sec. 5.

Fig. 4 shows for SNR < 20 dB Teager energy of signal becomes negative and the basic condition of the DESA-1 algorithm is not established.

6.2 Effect of outliers

An outlier is any value that is numerically distant from the rest of the data. The outliers can lead to inaccurate data processing and system identification. The Ref. (Amini and Ghasemi 2018) has investigated the effect of outliers on

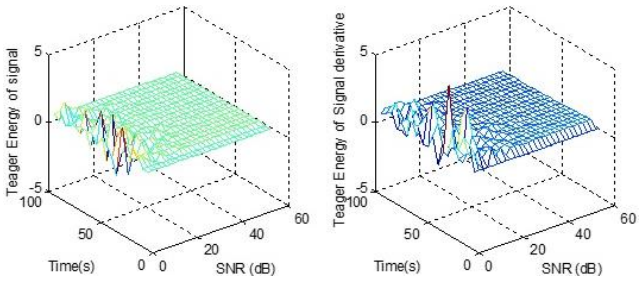

Fig. 4 Outputs of Teager energy operator for the signal and its derivative with respect to noises

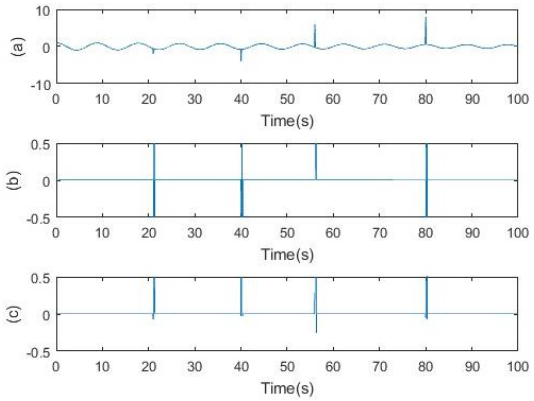

Fig. 5 Outputs of Teager energy operator for the signal and its derivative with respect to outliers. (a) shows the signal corrupted with outliers, (b) and (c) show Teager energy of signal and Teager energy of signal derivative, respectively

ESAI algorithm. It is found, the EASI algorithm is sensitive to presence of outliers.

In the DESA-1 algorithm, the outliers have same effect like noises and deteriorate the algorithm mainly due to the differentiators working over a very short time window. To investigate this issue, it is assumed that the signal introduced in the previous section is corrupted with outliers. The following data are added to the signal as outliers $[(210,-2),(400,-4),(560,6),(800,8)]$. First pair and second pair of added data represent the time and magnitude of outliers, respectively.

As shown in Fig. 5, at the points where there is an outlier, outputs of TEO for signal or its derivative become negative and the performance of the DESA-1 deteriorates. Therefore, the DESA-1 algorithm is sensitive to outliers. Because of EASI and DESA-1 algorithms' sensitivity to outlier presence, it is necessary to remove the outliers before separation. A good solution to remove outliers is to use median filter as pre-processing step. Median filter reduces the noise and outliers effectively. In this paper, three-point median filter is used to pre-process the separate and estimate.

7. Proposed method

This study combines the advantages of both EASI, which can perform signal source separation, and TEO (DESA-1), proposing a structural identification EASI-Teager method. The main steps of proposed method are illustrated in Fig. 6.

8. Simulation study

For the object of evaluating the performance of the proposed method, numerical simulations are performed on a simple shear building model with two story. For convenience, the damping is assumed to be mass proportional, see Fig. 7. The effectiveness investigation is carried out in two main stages. Firstly modal shapes and modal coordinates are extracted by EASI algorithm then modal parameters are estimated by DESA-1 from outputs of EASI.

The equations of motion for this system follow Eq. (1). It is assumed that $m_1 = 1\,Kg, m_2 = 2\,Kg$ and $k_1 = k_2 = 1\,N/m$. Also, similar damping ratio for all modes equal one percent is considered for simulation. The natural frequencies for mentioned building are $\omega = [1.3066, 0.5412]$. For free vibration, the initial displacements and velocities are considered $\mathbf{x}(0) = [1,0]^T$ and $\mathbf{v}(0) = [0,0]^T$, respectively. The displacements are corrupted by outliers. For forced vibration, Gaussian white noise is applied to each floor as random excitation. The time step in the simulation is 0.1 seconds, and a total time of 197 seconds is considered.

Obtained mode shapes are compared using a correlation coefficient known as the Modal Assurance Criterion (MAC) (Zarzoso and Nandi 2000). MAC values vary between 0 and 1, where a value of 1 means a perfect correlation. MAC is defined as Eq. (25)

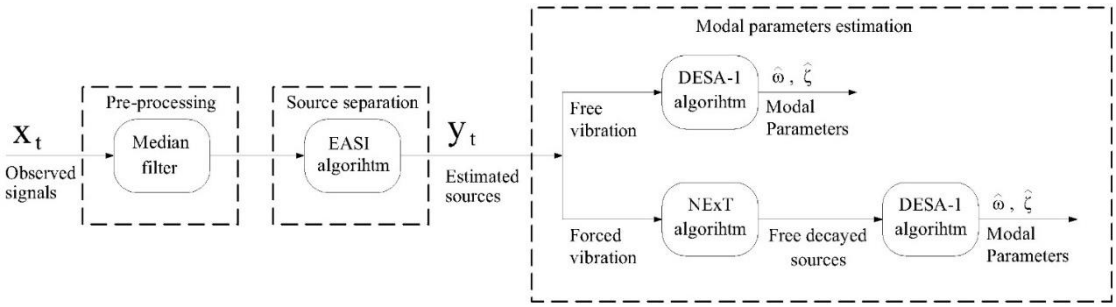

Fig. 6 The main steps of EASI-Teager method

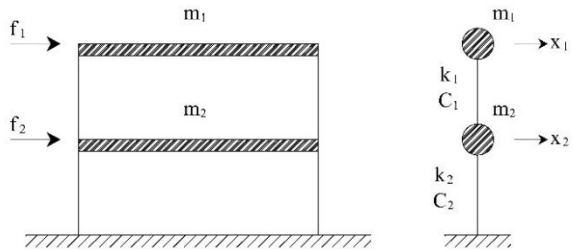

Fig. 7 A two story shear building model

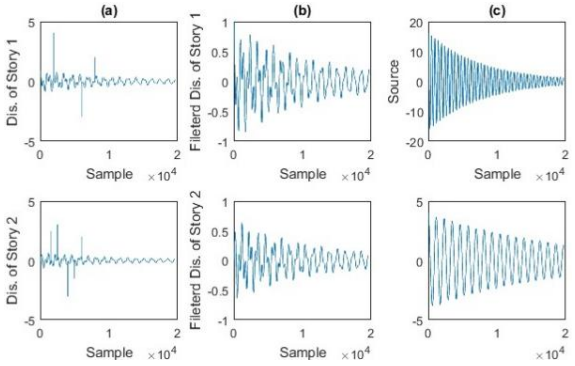

Fig. 8 Plots (a): displacement of the structure; plots (b): displacement of the structure after removing outliers by median filter; plots (c): separated sources by EASI. (Free vibration)

$$\mathrm{MAC}_i = \frac{(\boldsymbol{\varphi}_i^T \widehat{\boldsymbol{\varphi}}_i)^2}{(\boldsymbol{\varphi}_i^T \boldsymbol{\varphi}_i)(\widehat{\boldsymbol{\varphi}}_i^T \widehat{\boldsymbol{\varphi}}_i)} \tag{25}$$

Where $\boldsymbol{\varphi}_i$ and $\widehat{\boldsymbol{\varphi}}_i$ represent ith theoretical and estimated mode vectors, respectively.

In addition, the Euclidian distance of two mode shape vectors, Er is used to assess accuracy of separation.

$$\mathrm{Er}_i = \|\boldsymbol{\varphi}_i - \widehat{\boldsymbol{\varphi}}_i\|_2 \tag{26}$$

8.1 Free vibration system

In the free vibration case, there is no external force applied to the system. At first, according to sensitivity of EASI algorithm to outliers, before separation, median filter is applied to remove outliers. Fig. 8 illustrates the system response contaminated with the outliers, the responses after removing outliers and the sources identified by EASI.

The next step after separation is to determine the modal parameters by means of the DESA-1 algorithm. The results of separation and identification are illustrated in Table 3.

8.2 Forced vibration system

For investigation of the forced vibration case, the Gaussian white noise is considered as the stationary random excitations applied to the system. The identification is performed for 100 different $\mathbf{f}(t)$ samples. The parameters presented in Table 4. are the mean value of acceptable identification when the MAC of each identified mode is greater than 0.90 and the obtained modal parameters are real.

Table 3 Accuracy of the separation using EASI and identification by DESA-1 for free vibration of the 2-DOF system

Step	Method	Mode 1		Mode 2	
		MAC_1	Er_1	MAC_2	Er_2
Separation	EASI	1.0000	0.0001	0.9989	0.032
		$\widehat{\omega}_1$	$\hat{\zeta}_1(\%)$	$\widehat{\omega}_2$	$\hat{\zeta}_2(\%)$
Identification	DESA-1	1.3056	0.010	0.5394	0.011
	HT	1.3065	0.010	0.5414	0.009

Table 4 Accuracy of the separation using EASI and identification by DESA-1 for forced vibration of the 2-DOF system

Step	Method	Mode 1		Mode 2	
		MAC_1	Er_1	MAC_2	Er_2
Separation	EASI	0.9972	0.0316	0.9933	0.0677
		$\widehat{\omega}_1$	$\hat{\zeta}_1(\%)$	$\widehat{\omega}_2$	$\hat{\zeta}_2(\%)$
Identification	DESA-1	1.3128	0.010	0.5423	0.013
	HT	1.3087	0.0082	0.5428	0.019

It should be noted, for forced vibration state, the extracted sources are not exponentially damped sinusoid like free vibration.

This is displayed in Fig. 9 for a sample excitation, (SeedNum = 23 in MATLAB). This issue complicates the identification. To overcome this problem, the Next algorithm is applied to transform forced responses to free decays, see Fig. 9. Then the DESA-1 is used to estimate the modal parameters easily. For all identification samples, the source related to first mode is considered as references signal.

As seen in the Table 4. the EASI algorithm has separated the responses well. The both of HT and DESA-1 algorithms have good performance in identification of parameters but the DESA-1 is better.

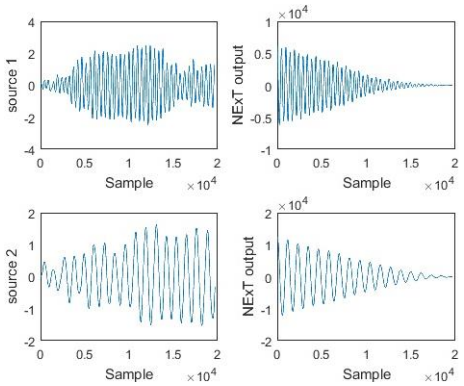

Fig. 9 Left: separated sources by EASI; Right: Appling NExT algorithm on sources (SeedNum = 23)

Table 5 Accuracy of the separation using EASI and identification by DESA-1 for noisy free vibration of the 2-DOF system

SNR (dB)	Separation				Identification			
	Mode 1		Mode 2		Mode 1		Mode 2	
	MAC	Er	MAC	Er	$\hat{\omega}_1$	$\hat{\zeta}_2$(%	$\hat{\omega}_1$	$\hat{\zeta}_2$(%
60	1.0000	0.0001	0.9988	0.0350	1.3076	0.010	0.5425	0.010
40	1.0000	0.0003	0.9989	0.0330	1.3035	0.009	0.5388	0.008
20	0.9999	0.0040	0.9826	0.0500	1.3131	0.010	0.5324	0.011
15	0.9989	0.0625	0.9772	0.0918	1.3221	0.012	0.5521	0.015
12.5	0.9972	0.0845	0.9726	0.1029	N/A	N/A	N/A	N/A
10.0	0.9954	0.1036	0.9438	0.2158	N/A	N/A	N/A	N/A
9.5	0.9728	0.1598	0.9265	0.4215	N/A	N/A	N/A	N/A
8.5	0.9556	0.2684	N/A	N/A	N/A	N/A	N/A	N/A
7.5	0.9202	0.3576	N/A	N/A	N/A	N/A	N/A	N/A

8.3 The effect of noise on EASI-Teager method

To study the performance of the proposed method in the presence of noise, the outputs of free vibration case are corrupted by white Gaussian noise. The signal-to-noise ratios (SNRs) considered are 7.5, 8.5, 9.5, 10, 12.5, 15, 20, 40, 60 dB for investigation. The simulation is undertaken for 100 different samples. Given that the robustness of the proposed method against noise is affected by the robustness of the EASI and DESA-1 algorithms together. Thus, their performance are investigated separately. Results presented in Table 5. shows, adaptive blind source separation (ABBS) method is insensitive to noise and for $SNR > 9.5$ it has been able to separate sources well. For $15.0 \leq SNR$, both DESA-1 and EASI algorithms have good performance. for $9.5 \leq SNR < 15.0$, separation by the EASI algorithm still remains accurate but separated sources are very noisy and DESA-1 algorithm does not works for this range. For $SNR < 9.5$, both EASI and DESA-1 algorithms fail. As a results, the performance of the proposed method is limited to SNR more than 15.0.

9. UBC benchmark structure simulation

At the 1996 international workshop on structural control, the International Association for Structural Control (IASC) created task groups to study the problem of structural health monitoring of civil structures.

In this section, the first phase of this study, based on simulated response of a test structure is used to compare performances of various algorithms of modal parameters identification (Lus *et al*. 2004).

The IASC-ASCE structure is located at the earthquake engineering research laboratory of the University of British Columbia. As shown in Fig. 10 it is a four-story 2-bay by 2-bay steel frame with 2.5 m × 2.5 m base, and 3.6 m tall. Details of the benchmark problem, including masses, stiffness and other specifications is given in reference (Johnson *et al*. 2004).

The structure is modeled as a 12-DOF system with three DOFs per floor (two translations in x and y, and one rotation) and by assuming that the floor slabs are rigid in and out of the plane. But in order to maintain symmetry, the structure model is considered as a 4-DOF shear-beam model.

For identification purposes, two damage patterns for case one are studied in this section. The undamaged case has already been studied by the authors in their previous work (Amini and Ghasemi 2018). These two damage patterns are depicted in Fig. 11, and are defined as follows:

(i) All braces in the first story are removed,
(ii) All braces in both first and third stories are removed.

The excitations are modeled as independent Gaussian

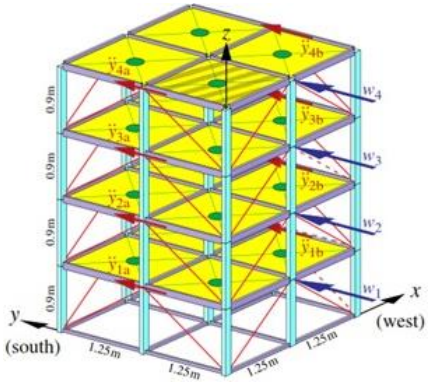

Fig. 10 Analytical model of UBC benchmark building

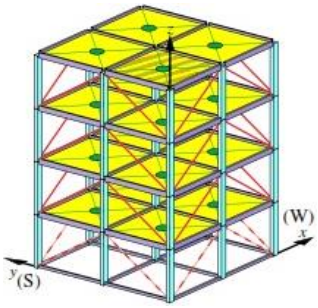

Damage pattern (i): no stiffness in 1^{st} floor braces

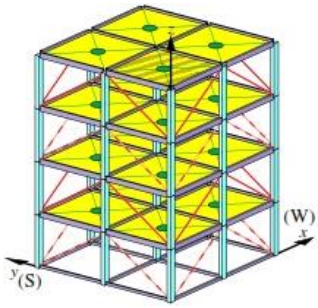

Damage pattern (ii): no stiffness in 1^{st} and 3^{rd} floors braces

Fig. 11 Considered damage patterns for UBC building

white noise to simulate the ambient vibration. They are applied to each floor in the weak direction (y-direction).

The random excitation records are 200 seconds long and the acceleration responses are measured at a sample rate of 200 Hz. The measured responses in two noise-free and noisy states will be used for system identification purposes. For the noisy case, the acceleration responses were corrupted with 10% RMS of each floor response. In spite of the fact that, in this benchmark, the acceleration responses are batch, but in order to simulate online identification, it is assumed new data is recorded for each time. For simplicity and considering the limits of EASI, normal modes are assumed to exist and the damping ratio is assumed to be zero for all modes (Amini and Ghasemi 2018). For effective implementation of NExT algorithm, the acceleration of the fourth separated source is selected as reference signal (Caicedo *et al*. 2004). 20 different excitation samples are selected for identification. So the MACs, error values and estimated natural frequencies and damping ratios are therefore the mean values of the acceptable identifications.

9.1 Damage pattern (i)

Tables 6-7 illustrate the modal identification results containing natural frequencies and damping ratios for damage pattern (i) in noise free and noisy cases, respectively.

In order to improve the performance of DESA-1 algorithm and considering the effect of previous data, an average of the last 5 steps are used in the estimation of parameters at each time. Then, the modal parameters are calculated as Eq. (27).

Table 6 Extracted modal parameters of IASC-ASCE benchmark building for damage pattern (i) and noise free case

Modes	MAC	Er	Frequency (Hz)			Damping ratio (%)		
			Theo.	Est.		Theo.	Est.	
				DESA-1	HT		DESA-1	HT
1	0.9877	0.0860	6.24	6.26	6.18	0.000	0.005	0.002
2	0.9882	0.0796	21.53	21.56	21.54	0.000	0.026	0.010
3	0.9999	0.0092	37.37	37.47	37.39	0.000	0.003	0.008
4	0.9855	0.0803	47.83	47.86	47.85	0.000	0.009	0.006

Table 7 Extracted modal parameters of IASC-ASCE benchmark building for damage pattern (i) and the noisy case

Modes	MAC	Er	Frequency (Hz)			Damping ratio (%)		
			Theo.	Est.		Theo.	Est.	
				DESA-1	HT		DESA-1	HT
1	0.9963	0.0475	6.24	6.52	6.49	0.000	0.022	0.034
2	0.9847	0.0888	21.53	21.55	21.54	0.000	0.017	0.008
3	0.9883	0.0778	37.37	37.38	37.39	0.000	0.000	0.006
4	0.9827	0.0924	47.83	47.86	47.85	0.000	0.007	0.004

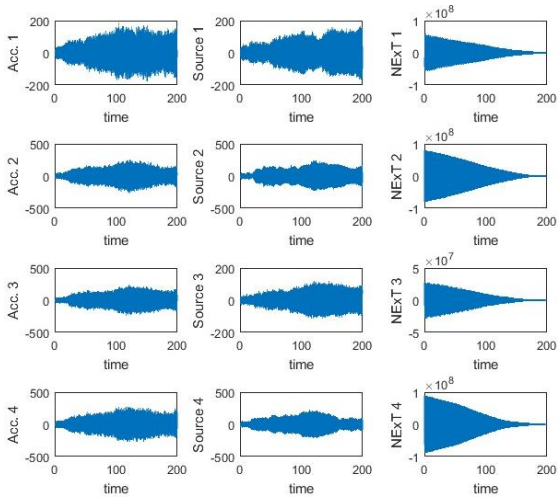

Fig. 12 Acceleration responses, extracted sources by EASI and outputs of NExT algorithm for the noisy cases of damage pattern (i) (SeedNum = 319)

$$\overline{\omega_n} = \frac{1}{5}\left(\sum_{n-5}^{n} \omega_i\right), \qquad \overline{\zeta_n} = \frac{1}{5}\left(\sum_{n-5}^{n} \zeta_i\right) \tag{27}$$

Where ω_i and ζ_i are modal parameters at ith step. So, $\overline{\omega_n}$ and $\overline{\zeta_n}$ are considered as modal parameters at each time. As seen in the tables, the EASI algorithm performs well in identifying mode shapes and separating sources. In addition, there is good agreement between both exact and estimated parameters by DESA-1 and HT algorithms.

Fig. 12 shows the acceleration responses, extracted sources by EASI and outputs of NExT algorithm for damage pattern (i) for a sample excitation (SeedNum = 319 in MATLAB) in the noisy case.

9.2 Damage pattern (ii)

The results of estimated natural frequencies and damping ratios for damage patterns (ii) in noise free and noisy cases are presented in Tables 8-9. The results show the good efficacy of the EASI algorithm in identifying mode shapes and sources. Similar to previous damage pattern, the HT and DESA-1 algorithms have a good performance in identifying modal parameters. Also, the

Table 8 Extracted modal parameters of IASC-ASCE benchmark building for damage pattern (ii) and noise free case

Modes	MAC	Er	Frequency (Hz)			Damping ratio (%)		
			Theo.	Est.		Theo.	Est.	
				DESA-1	HT		DESA-1	HT
1	0.9902	0.0666	5.82	6.10	5.87	0.000	0.000	0.031
2	0.9912	0.0547	14.89	14.87	14.89	0.000	0.021	0.012
3	0.9968	0.338	36.06	36.08	0.000	0.000	0.008	0.006
4	0.9877	0.0694	41.35	41.33	41.37	0.000	0.007	0.007

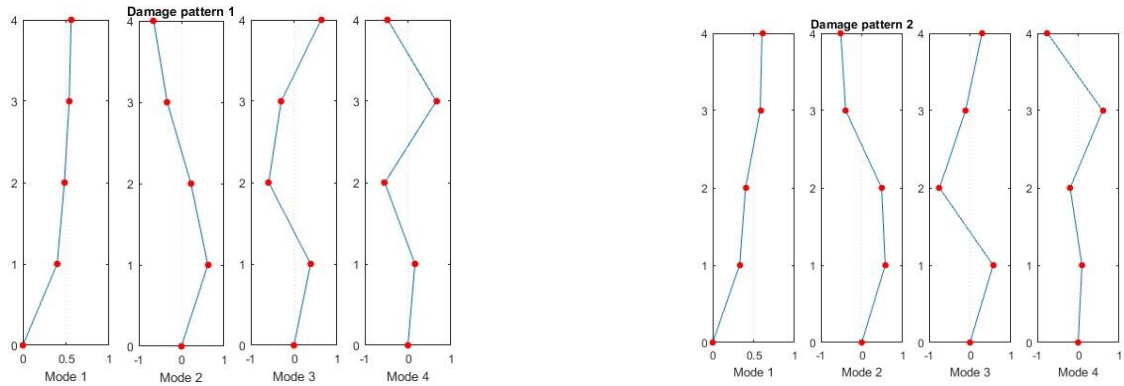

Damage pattern (i) Damage pattern (ii)

Fig. 13 The mode shapes of UBC building for damage patterns

Table 9 Extracted modal parameters of IASC-ASCE benchmark building for damage pattern (ii) and the noisy case

Modes	MAC	Er	Frequency (Hz)			Damping ratio (%)		
			Theo.	Est.		Theo.	Est.	
				DESA-1	HT		DESA-1	HT
1	0.9849	0.1619	5.82	6.02	5.82	0.000	0.0001	0.0002
2	0.9912	0.0644	14.89	14.87	14.82	0.000	0.0007	0.0001
3	0.9854	0.0882	36.06	36.14	36.05	0.000	0.0005	0.0000
4	0.9824	0.0931	41.35	41.32	41.37	0.000	0.0002	0.0000

estimated modal parameters using the DESA-1 algorithm are very close to exact values. Fig. 13 presents the extracted mode shapes for damage patterns (i) and (ii) in the noisy case. It should be noted that similar results were obtained for the noise free case.

10. Conclusions

This paper has presented the conjunction of equivariant adaptive separation via independence (EASI) and Teager Energy Operator (TEO) called EASI-Teager approach for online identification of structural modal parameters. The EASI algorithm is an adaptive blind source separation method, updates the separating matrix and sources in each time. In this proposed method, in the first step, the EASI algorithm is applied to structural responses to extract modal matrix and modal coordinates as independent sources. In the second step, the instantaneous frequencies and damping ratios are estimated from separated modal coordinates using TEO based demodulation method, discrete energy separation algorithm (DESA-1). In forced vibration state, the extracted sourced are not exponentially damped sinusoid. To simplify the identification, before applying the DESA-1 algorithm, the NExT algorithm is used for transferring forced responses to free decays.

The effects of noise and outliers on the operation of the DESA-1 are investigated in this research. This algorithm is very sensitive with respect to presence of noise and outliers due to its high resolution. Depending on the amount of noise, it may deteriorate the DESA-1 efficiency.

Consequently, in order to achieve accurate results, median filter is used to remove outliers from the data.

The effectiveness of the proposed approach has been investigated using a synthetic example. For both free vibration and forced vibration states, the EASI has good performance. Also, both of DESA-1 and HT methods can estimate modal parameters well.

The phase I IASC-ASCE benchmark building has been used for verification of this method as well. The successful modal identification results demonstrate that the EASI-Teager algorithm is efficient and proper for online structural identification.

References

Abazarsa, F., Nateghi, F., Ghahari, S.F. and Taciroglu, E. (2016), "Extended blind modal identification technique for nonstationary excitations and its verification and validation", *J. Eng. Mech.*, **142**(2), 04015078. https://doi.org/10.1061/(ASCE)EM.1943-7889.0000990

Amini, F. and Ghasemi, V. (2018), "Adaptive modal identification of structures with equivariant adaptive separation via independence approach", *J. Sound Vib.*, **413**, 66-78. https://doi.org/10.1016/j.jsv.2017.09.033

Azam, S.E. and Mariani, S. (2018), "Online damage detection in structural systems via dynamic inverse analysis: A recursive Bayesian approach", *Eng. Struct.*, **159**, 28-45. https://doi.org/10.1016/j.engstruct.2017.12.031

Azam, S.E., Attari, N.K.A. and Mariani, S. (2017), "Online damage detection via a synergy of proper orthogonal decomposition and recursive Bayesian filters", *Nonlinear Dyn.*, **89**(2), 1489-1511. https://doi.org/10.1007/s11071-017-3530-1

Azergui, M., Abenaou, A. and Bouzahir, H. (2018), "A Teager-Kaiser Energy Operator and Wavelet Packet Transform for Bearing Fault Detection", *Smart Science*, **6**(3), 227-233. https://doi.org/10.1080/23080477.2018.1460892

Caicedo, J.M., Dyke, S.J. and Johnson, E.A. (2004), "Natural excitation technique and eigensystem realization algorithm for phase I of the IASC-ASCE benchmark problem: Simulated data", *J. Eng. Mech.*, **130**(1), 49-60. https://doi.org/10.1061/(ASCE)0733-9399(2004)130:1(49)

Cao, M., Radzieński, M., Xu, W. and Ostachowicz, W. (2014), "Identification of multiple damages in beams based on robust curvature mode shapes", *Mech. Syst. Signal Process.*, **46**(2), 468-480. https://doi.org/10.1016/j.ymssp.2014.01.004

Cardoso, J.-F. and Laheld, B.H. (1996), "Equivariant adaptive source separation", *IEEE Transection Signal Process*., **44**(2), 3017-3030. https://doi.org/10.1109/78.553476

Chase, J.G., Begoca, V. and Barroso, L. (2005a), "Efficient structural health monitoring for a benchmark structure using adaptive RLS filters", *Comput*. *Struct*., **83**(8-9), 639-647. https://doi.org/10.1016/j.compstruc.2004.11.005

Chase, J.G, Leo Hwang, K., Barroso, L.R. and Mander, J.B. (2005b), "A simple LMS-based approach to the structural health monitoring benchmark problem", *J. Earthq*. *Eng*. *Struct*. *Dyn*. (*EESD*), **34**(6), 575-594. https://doi.org/10.1002/eqe.433

Chu, S.-Y. and Lo, S.-C, (2011), "Application of the on-line recursive least-squares method to perform structural damage assessment", *Struct*. *Control Health Monit*., **18**(3), 241-264. https://doi.org/10.1002/stc.362

Comon, P. (1989), "Separation of stochastic processes", *Proceedings of the Workshop Higher Order Spectral Analaysis*, Vail, CO, USA, pp. 174-179. https://doi.org/10.1109/HOSA.1989.735291

Dimitriadis, D. and Maragos, P. (2006), "Continuous energy demodulation methods and application to speech analysis", *Speech Commun*., **48**(7), 819-837. https://doi.org/10.1016/j.specom.2005.08.007

Feldman, M. (2011), "Hilbert transform in vibration analysis", *Mech*. *Syst*. *Signal Process*., **25**(3), 735-802. https://doi.org/10.1016/j.ymssp.2010.07.018

Ghahari, S.F., Abazarsa, F. and Taciroglu, E. (2017), "Blind modal identification of non-classically damped structures under non-stationary excitations", *Struct*. *Control Health Monit*., **24**(6), e1925. https://doi.org/10.1002/stc.1925

Guo, Y. and Kareem, A. (2016a), "System identification through nonstationary data using time-frequency blind source separation", *J. Sound Vib*., **371**, 110-131. https://doi.org/10.1016/j.jsv.2016.02.011

Guo, Y. and Kareem, A. (2016b), "Non-stationary frequency domain system identification using time-frequency representations", *Mech*. *Syst*. *Signal Process*., **72-73**, 712-726. https://doi.org/10.1016/j.ymssp.2015.10.031

Hazra, B., Roffel, A.J., Narasimhan, S. and Pandey, M.D. (2010), "Modified cross-correlation method for the blind identification of structures", *J. Eng*. *Mech*., **136**(7), 889-897. https://doi.org/10.1061/(ASCE)EM.1943-7889.0000133

James, G.H., Carne, T.G. and Lauffer, J.P. (1993), "The natural excitation technique for modal parameter extraction from operating wind turbines", *Int*. *J*. *Anal*. *Experim*. *Modal Anal*., **10**(4).

Johnson, E.A., Lam, H.F., Katafygiotis, L.S. and Beck, J.L. (2004), "Phase I IASC-ASCE structural health monitoring benchmark problem using simulated data", *J. Eng*. *Mech*., **130**(1), 3-15. https://doi.org/10.1061/(ASCE)0733-9399(2004)130:1(3)

Jutten, C. and Herault, J. (1991), "Blind separation of sources, part I: An adaptive algorithm based on neuromimetic architecture", *Signal Process*., **24**(1), 1-10. https://doi.org/10.1016/0165-1684(91)90079-X

Kaiser, J.F. (1990), "On a simple algorithm to calculate the 'energy' of a signal", *Proceedings of IEEE ICASSP-90*, Albuquerque, NM, USA, April. https://doi.org/10.1109/ICASSP.1990.115702

Kaiser, J. (1993), "Some useful properties of Teager's energy operators", *Proceedings of IEEE International Conference on Acoustics*, *Speech*, *and Signal Processing*, Minneapolis, MN, USA, May. https://doi.org/10.1109/ICASSP.1993.319457

Lagunas Hernandez, M.A. (1994), "A general adaptive algorithm for nongaussian source separation without any constraint", *Proceedings of EUSIPCO-94*, *7th European Signal Processing Conference*, Edinburgh, UK, pp. 1161-1164.

Liang, M. and Bozchalooi, I.S. (2010), "An energy operator approach to joint application of amplitude and frequency-demodulations for bearing fault detection", *Mech*. *Syst*. *Signal Process*., **24**(5), 1473-1494. https://doi.org/10.1016/j.ymssp.2009.12.007

Loh, C.H., Weng, J.H., Liu, Y.C., Lin, P.Y. and Huang, S.K. (2011), "Structural damage diagnosis based on on-line recursive stochastic subspace identification", *Smart Mater*. *Struct*., **20**(5). https://doi.org/10.1002/stc.362

Loh, C.-H., Liu, Y.-C. and Ni, Y.-Q. (2012), "SSA-based stochastic subspace identification of structures from output-only vibration measurements", *Smart Struct*. *Syst*., *Int*. *J*., **10**(4), 331-351. https://doi.org/10.12989/sss.2012.10.4_5.331

Lus, H., Betti, R., Yu, J. and De Angelis, M. (2004), "Investigation of a system identification methodology in the context of the ASCE benchmark problem", *J. Eng*. *Mech*., **130**(1), 71-84. https://doi.org/10.1061/(ASCE)0733-9399(2004)130:1(71)

Maragos, P., Kaiser, J. and Quatieri T. (1993), "Energy separation in signal modulations with application to speech analysis", *IEEE Transactions on Signal Process*., **41**(10), 3024-3051. https://doi.org/10.1109/78.277799

McNeill, S.I. and Zimmerman, D.C. (2008), "A framework for blind modal identification using joint approximate diagonalization", *Mech*. *Syst*. *Signal Process*., **22**(7), 1526-1548. https://doi.org/10.1016/j.ymssp.2008.01.010

Nagarajaiah, S. and Yang, Y. (2015), "Blind modal identification of output-only non-proportionally-damped structures by time-frequency complex independent component analysis", *Smart Struct*. *Syst*., *Int*. *J*., **15**(1), 81-97. https://doi.org/10.12989/.2015.15.1.081

Poncelet, F., Kerschen, G. and Golinval, J.-C. (2007), "Output-only modal analysis using blind source separation techniques", *Mech*. *Syst*. *Signal Process*., **21**(6), 2335-2358. https://doi.org/10.1016/j.ymssp.2006.12.005

Rageh, A., Azam, S.E. and Linzell, D.G. (2020), "Steel railway bridge fatigue damage detection using numerical models and machine learning: Mitigating influence of modeling uncertainty", *Int*. *J*. *Fatigue*, **134**, 105458. https://doi.org/10.1016/j.ijfatigue.2019.105458

Rainieri, C. (2014), "Perspectives of Second-Order Blind Identification for Operational Modal Analysis of Civil Structures", *Shock Vib*., Article ID 845106, 9 pages. https://doi.org/10.1155/2014/845106

Ramazani, S. and Bahar, O. (2015), "EMD-based output-only identification of mode shapes of linear structures", *Smart Struct*. *Syst*., *Int*. *J*., **16**(5), 919-935. https://doi.org/10.12989/sss.2015.16.5.919

Sadhu, A., Hazra, B. and Narasimhan, S. (2014), "Ambient modal identification of structures equipped with tuned mass dampers using parallel factor blind source separation", *Smart Struct*. *Syst*., *Int*. *J*., **13**(2), 257-280. https://doi.org/10.12989/sss.2014.13.2.257

Sadhu, A., Prakash, G. and Narasimhan, S. (2016), "A hybrid hidden Markov model towards fault detection of rotating components", *J. Vib*. *Control*, **23**(19), 3175-3195. https://doi.org/10.1177/1077546315627934

Samadi, S., Babaie-Zadeh, M., Jutten, C. and Nayebi, K. (2004), "Blind source separation by adaptive estimation of score function difference", *Proceedings of the 5th International Conference on Independent Component Analysis and Blind Signal Separation*, Granada, Spain, pp. 22-24. https://doi.org/10.1007/978-3-540-30110-3_2

Santos, A., Figueiredo, E., Silva, M.F.M., Sales, C.S. and Costa, J.C.W.A. (2016), "Machine learning algorithms for damage detection: Kernel-based approaches", *J. Sound Vib*., **363**, 584-599. https://doi.org/10.1016/j.jsv.2015.11.008

Song, M., Astroza, R., Ebrahimian, H., Moaveni, B. and

Papadimitriou, C. (2020), "Adaptive Kalman filters for 12nonlinear finite element model updating", *Mech. Syst. Signal Process*, **143**, 106837. https://doi.org/10.1016/j.ymssp.2020.106837

Sorouchyari, E. (1991), "Blind separation of sources, part III: Stability analysis", *Signal Process.*, **24**(1), 21-29. https://doi.org/10.1016/0165-1684(91)90081-S

Ulriksen, M.D. and Damkilde, L. (2016), "Structural damage localization by outlier analysis of signal-processed mode shapes - Analytical and experimental validation", *Mech. Syst. Signal Process.*, **68-69**, 1-14. https://doi.org/10.1016/j.ymssp.2015.07.021

Ye, J. and Jin, H. (2009), "An optimized EASI algorithm", *Signal Process.*, **89**(3), 333-338. https://doi.org/10.1016/j.sigpro.2008.08.015

Zarzoso, V. and Nandi, A.K. (2000), "Adaptive blind source separation for virtually any source probability density function", *IEEE Transection Signal Process.*, **48**, 477-488. https://doi.org/10.1109/78.823974

HJ